PHYSICAL REVIEW B **75**, 153102 (2007)

# Nature of electronic states at the Fermi level of metallic $\beta$-$PbO_2$ revealed by hard x-ray photoemission spectroscopy

D. J. Payne,[1] R. G. Egdell,[1,*] G. Paolicelli,[2] F. Offi,[3] G. Panaccione,[4] P. Lacovig,[5] G. Monaco,[6] G. Vanko,[6] A. Walsh,[7]
G. W. Watson,[7] J. Guo,[8] G. Beamson,[9] P.-A. Glans,[10] T. Learmonth,[10] and K. E. Smith[10]
[1]*Inorganic Chemistry Laboratory, South Parks Road, Oxford OX1 3QR, United Kingdom*
[2]*CNR-INFM, National Research Center S3, Via Campi 213/a, I-41100 Modena, Italy*
[3]*CNISM and Dipartimento di Fisica, Università Roma Tre, Via della Vasca Navale 84, I-00146 Roma, Italy*
[4]*Laboratorio TASC, INFM-CNR, Area Science Park, S.S. 14, Km 163.5, 34012 Trieste, Italy*
[5]*Sincrotrone Trieste, S.C.p.A., S.S. 14, Km 163, Area Science Park, I-34012 Trieste, Italy*
[6]*European Synchrotron Radiation Facility, Boite Postal 220, 38042 Grenoble Cedex 9, France*
[7]*School of Chemistry, Trinity College, Dublin 2, Ireland*
[8]*Advanced Light Source, Lawrence Berkeley National Laboratory, Berkeley, California 94720, USA*
[9]*NCESS, Daresbury Laboratory, Warrington, Cheshire WA4 4AD, United Kingdom*
[10]*Department of Physics, Boston University, 590 Commonwealth Avenue, Boston, Massachusetts 02215, USA*
(Received 9 November 2006; revised manuscript received 2 February 2007; published 17 April 2007)

The nature of electronic states at the Fermi energy in metallic $\beta$-$PbO_2$ has been identified by hard x-ray photoemission spectroscopy (HXPS) combined with x-ray emission spectroscopy and density-functional theory calculations. Pb 6*s* states are strongly enhanced in HXP spectra, allowing us to locate the Fermi level above the top of the valence band. The occupied conduction-band states have significant Pb 6*s* character, although the major 6*s* contribution to the density of states is found 9 eV below the Fermi energy. The enormous potential of HXPS for the study of *s* states in oxides is emphasized.

DOI: 10.1103/PhysRevB.75.153102 PACS number(s): 78.70.En, 79.60.−i

Almost all binary dioxides where the metal atom achieves the group oxidation state are insulators with an energy gap of at least 3 eV separating a filled valence band of states with dominant O 2*p* atomic character from an empty conduction band of cation states. Examples include $TiO_2$, $ZrO_2$, $HfO_2$, $ThO_2$, $GeO_2$, and $SnO_2$.[1,2] By contrast, $\beta$-$PbO_2$ is a metallic conductor.[3,4] The metallic nature of $\beta$-$PbO_2$ is therefore unique within this class of materials and is at present incompletely understood. The high conductivity of $\beta$-$PbO_2$ is in turn of wide significance because lead dioxide is the medium for storage of chemical energy on the cathode plate of lead-acid batteries.[5] Crucial to the ability of these batteries to deliver the high currents needed to turn over the starter motor of an internal combustion engine is the fact that the cathode coating in the charged state does not contribute significantly to the internal resistance of the battery. The unexpected metallic conductivity of $\beta$-$PbO_2$ is therefore both of fundamental physical interest and of enormous technological importance.

What is the nature of the electronic states close to the Fermi level in $\beta$-$PbO_2$? In the simplest textbook description, $PbO_2$ has a filled valence band of O 2*p* states and an empty conduction band of Pb 6*s* states. Earlier band-structure calculations have suggested that the metallic behavior is an intrinsic property of the stoichiometric rutile phase of $\beta$-$PbO_2$ due to overlap of the bottom of the conduction band with the top of the valence band.[6] On the other hand, the carrier concentration varies with preparation conditions in a way suggestive of occupation of conduction-band states by carriers introduced by donor defects.[7] In the present Brief Report, it is shown that the Fermi level in $\beta$-$PbO_2$ sits above the edge of the topmost valence band, consistent with the defect model. However, it emerges that it is incorrect to assume[8,9] that the metal *ns* states are concentrated near the Fermi energy in post-transition metal oxides. We come to these conclusions by studying $\beta$-$PbO_2$ with a combination of hard x-ray photoemission spectroscopy (HXPS), soft x-ray emission spectroscopy (XES), and density-functional theory (DFT) calculations. We show that the cross section for ionization of Pb 6*s* state is strongly enhanced at photon energies of 6000 or 7700 eV relative to the cross section for O 2*p* states and thus HXPS can be used as a probe of Pb 6*s* character in the filled states. At the same time, HXPS facilitates the study of technological samples due to the much longer electron path length[10] and correspondingly reduced surface sensitivity as compared with low-energy photoemission. Oxygen *K* shell emission gives a complementary view of the valence-band electronic structure sensitive only to O 2*p* states. With the combination of these two bulk sensitive techniques supported by DFT calculations, we find that the dominant Pb 6*s* contribution to the density of states is in a region about 9 eV below $E_F$. The partially populated conduction-band states also possess Pb 6*s* character. However, in contrast to simple expectations, the 6*s* contribution to conduction-band states is shown to be less than the contribution to the valence band. We argue that the combination of HXPS with element specific XES and density-functional calculations provides a uniquely powerful and completely general approach to the characterization of the bulk electronic structure of oxide materials and, in particular, of the distribution of metal *s* character.

Metallic films of $\beta$-$PbO_2$ with the tetragonal rutile structure were deposited on polished Pt substrates by anodic oxidation of solutions of $Pb(NO_3)_2$ in $HNO_3$ as described previously.[11] The nominal film thickness was 15 $\mu$m. The films were rinsed in ultrapure water and dried at 100 °C. The *n*-type carrier concentration in as-prepared films was estimated to be $1.1 \times 10^{21}$ cm$^{-3}$.[11] XES experiments were performed on beamline 7.0.1 at the Advanced Light Source, Lawrence Berkeley National Laboratory (USA). As in previous work on PbO,[12] the overall resolution was set at 0.7 eV on the O *K* edge. HXPS measurements were performed on beamline ID16 of the European Synchrotron Radiation Facility in Grenoble (France) using the spectrometer developed under the European Volume Photoemission project.[13,14] The overall instrument resolution was 0.35 and 0.25 eV, respectively, at 6000 and 7700 eV photon energy. Binding energies in the XPS experiments were referenced to the metallic Fermi edge of $\beta$-PbO$_2$ and the XES data were aligned relative to the XPS on the peak maxima. Adventitous carbon contamination in HXPS was minimal even without sample pretreatment, with a C 1*s*/O 1*s* intensity ratio below the level of detection at $h\nu$=7700 eV. Spectra were therefore measured at room temperature on "as-presented" samples. Typical spectral accumulation times for valence bands were around 6 h. The total accumulated counts (about 10 000 per channel on the strongest valence-band peak) and signal-to-noise ratio were very similar to those achieved in earlier offline XPS experiments[11] using a rotating anode Al $K\alpha$ x-ray source despite the fact that the absolute value for the O 2*p* ionization cross section is over 2 orders of magnitude smaller at 8000 eV photon energy than at 1486.6 eV (see below). The experimental data are compared with densities of states calculated using periodic DFT as embodied in the Vienna *ab initio* simulation package, as described previously.[11] The full and partial density of states profiles from the earlier work were convoluted with a Gaussian of full width at half maximum height of 0.8 eV to allow for phonon and instrument broadening in the experimental spectra. Phonon broadening in oxides is typically of the order of 1 eV, although in metallic PbO$_2$ we may expect a somewhat smaller broadening than is usual.[15]

The band-structure calculations show that the description of PbO$_2$ in terms of a valence band of O 2*p* states and a conduction band of Pb 6*s* states is not correct (Fig. 1). There is pronounced hybridization between O 2*p* and Pb valence states, and the Bader charge[16] on the Pb cations has a value of only +2.07. The valence band contains three features labeled I, II, and III in Fig. 1, while the conduction band breaks down into two components i and ii. The Pb 6*s* contribution to the density of states is split between the lower conduction band i and band III found at the bottom of the valence band. The Pb 6*s* contribution to the valence band is greater than that to the lower conduction band. Similarly, Pb 6*p* character is divided between middle valence band II and the upper conduction band ii. The upper valence band I is almost pure O 2*p*. In the calculations, there is no overlap between valence and conduction bands in the raw partial density of states, which drops to zero at the Fermi energy. However, the two bands touch and after convolution with a broadening function they appear to merge. Thus, $\beta$-PbO$_2$ is best described as a semimetal.

Using the combination of XES and valence-band HXPS, we are able to directly test the validity of the calculations. O $K\alpha$ XES and valence-band XPS of $\beta$-PbO$_2$ excited at 6000 and 7700 eV photon energies are shown in Fig. 2, with XPS data taken at $h\nu$=1486.6 eV (Ref. 11) also included for comparison. Due to strong dipole selection rules and the localized atomic nature of the x-ray emission process, the O $K\alpha$ emission spectrum is a direct measure of the O 2*p* partial density of states. The O $K\alpha$ emission spectrum is dominated by the valence-band feature I, consistent with the calculations which show that this band is primarily of O 2*p* character. Feature III in the XES data is extremely weak, reflecting the strong Pb 6*s* contribution and correspondingly reduced O 2*p* contribution to the density of states. However, in photoemission using 7700 eV excitation, peak III is the dominant feature in the valence-band spectrum. In addition, the intensity of feature II increases relative to that of feature I, but to a lesser extent than that of feature III. Spectra excited at the lower photon energies of 6000 and 1486.6 eV display relative intensities intermediate between the O *K* shell emission spectrum and the spectrum excited at $h\nu$ =7700 eV.

Qualitatively, these changes can be understood simply in terms of the fact that the cross sections for ionization of Pb 6*s* and Pb 6*p* states decay with increasing photon energy much less rapidly than the cross section for ionization of O 2*p* states (see cross sections calculated by Scofield[17] in Table I). These variations can, in turn, be understood in terms of the highly penetrating nature of the 6*s* and Pb 6*p* radial wave functions. Quantitatively, however, it seems that the Scofield tabulation overestimates the cross sections for ionization of Pb 6*s* and 6*p* orbitals relative to that of O 2*p*, particularly at high energy, so that the cross-section weighted density of states gives stronger spectral weight to peak III relative to peak I than is observed experimentally (cross sections calculated by Yeh and Lindau[18] using nonrelativistic Hartree-Fock theory are similarly at odds with the experi-

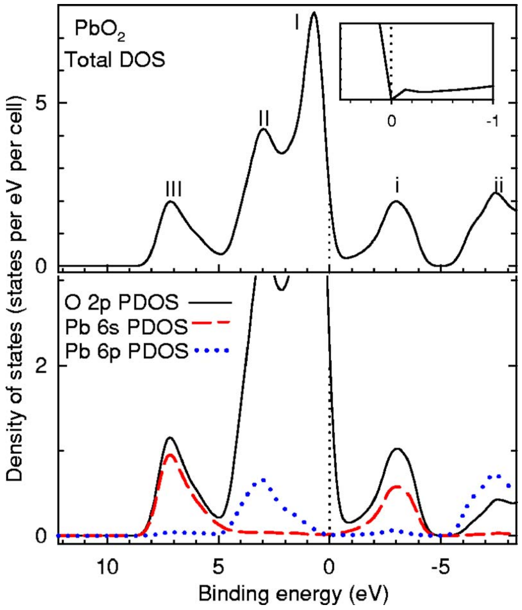

FIG. 1. (Color online) Total and partial densities of states for $\beta$-PbO$_2$ derived from band-structure calculations following convolution with a 0.8 eV Gaussian broadening function (see text). The inset shows the unbroadened full density of states. Energies are given relative to the Fermi energy for stoichiometric $\beta$-PbO$_2$.

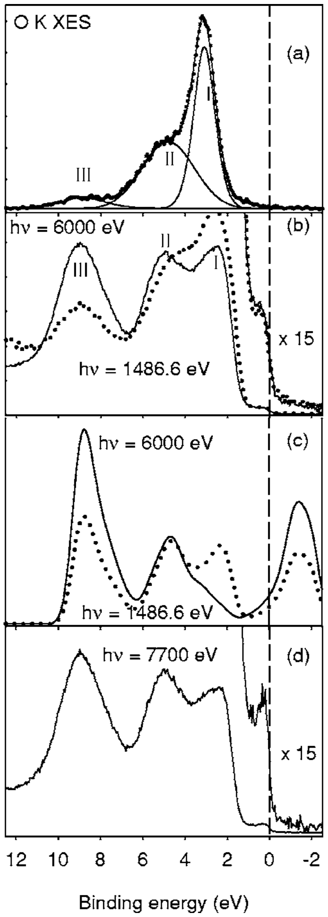

FIG. 2. (a) O $K$ shell x-ray emission spectrum of $\beta$-PbO$_2$. (b) HXPS excited at $h\nu$=6000 eV (solid line) with data at $h\nu$=1486.6 eV taken from Ref. 11 superimposed (dotted line). (c) Cross-section weighted densities of states derived from cross sections given in Ref. 16 at $h\nu$=6000 eV (solid line) and 1486.6 eV (dotted line). The Fermi level has been set 1.6 eV above the valence-band maximum to facilitate comparison with experimental data. (d) HXPS excited at $h\nu$=7700 eV.

mental data). This is illustrated in Fig. 2(c), which shows the cross-section weighted density of states calculated at 1486.6 and 6000 eV photon energies. Clearly, the calculated intensity of peak III in both Al $K\alpha$ XPS and HXPS is much too high relative to that of peak I. Further work is needed to establish why the computed cross sections are not quantitatively reliable.

TABLE I. One-electron cross section for ionization of valence orbitals of Pb and O derived from Dirac-Slater calculations (Ref. 16). All values are in barns. The figures in parentheses give cross sections for Pb 6$s$ and 6$p$ states relative to the O 2$p$ cross section.

| $h\nu$ (eV) | O 2$p$ | Pb 6$s$ | Pb 6$p$ |
|---|---|---|---|
| 1486.6 | $6.38\times10^{1}$ | $5.03\times10^{2}$<br>$(7.88\times10^{0})$ | $2.93\times10^{2}$<br>$(4.59\times10^{0})$ |
| 6000 | $3.17\times10^{-1}$ | $4.54\times10^{1}$<br>$(1.43\times10^{2})$ | $2.59\times10^{1}$<br>$(1.70\times10^{2})$ |
| 8000 | $1.00\times10^{-1}$ | $2.70\times10^{1}$<br>$(2.70\times10^{2})$ | $1.41\times10^{1}$<br>$(1.41\times10^{2})$ |

Al $K\alpha$ photoemission spectra of $\beta$-PbO$_2$ contain a weak feature about 1.6 eV above the top valence band, terminating in a sharp edge at the Fermi energy $E_F$. In parallel with the changes in the valence band, excitation of photoemission spectra at high photon energy leads to pronounced enhancement in the intensity of this structure close to $E_F$ relative to the peak at the top of the valence band. Under 7700 eV excitation, the low binding energy structure appears as a well-defined peak with a clear minimum between it and the main valence band—at lower photon energy, the structure appears only as a shoulder to the main valence band. These observations demonstrate that the metallic behavior of $\beta$-PbO$_2$ arises from partial filling of a conduction band that sits above the top of the main valence band. Occupation of the conduction band must arise from electron introduced donor states such as oxygen vacancy defects or proton interstitials. The observation that occupation of the conduction band increases from $1.1\times10^{21}$ to $2.0\times10^{21}$ cm$^{-3}$ after gentle annealing in UHV (Ref. 11) favors the vacancy hypothesis. The enhancement in the intensity of the conduction band in HXPS is consistent with the band-structure calculation, which shows the lower conduction band to have substantial Pb 6$s$ character. We can further analyze the intensity changes in relation to the computed partial densities of states. The valence states in band III have 55% O 2$p$ character and 45% Pb 6$s$ character. By contrast, the conduction-band states 1.6 eV above the top of the valence have 67% O 2$p$ character and only 33% Pb 6$s$ character. The reduced Pb 6$s$ contribution to the conduction band is reflected in the fact that although the peak at the Fermi energy increases in intensity relative to valence-band peak I (which relates to states of almost pure O 2$p$ character) on increasing the photon energy, the enhancement is *less* than for the valence-band peak III. Thus, the peak height at the Fermi energy *decreases* relative to that of peak III by about a factor of 2 over the photon energy range investigated.

In summary, we have shown that the intensity of structure associated with states that have pronounced metal 6$s$ character is strongly enhanced in the photoemission spectra of $\beta$-PbO$_2$ excited at high (7700 eV) photon energy. Further analysis of the intensity changes confirms that conduction-band states have less Pb 6$s$ character than the most tightly bound valence-band states, a conclusion in accord with band-structure calculations. Looking at the broader implications of the current work, cross sections for ionization of 4$s$ and 5$s$ orbitals are expected to be similar to those for 6$s$ orbitals at high energies.[17] It follows that selective enhancement of the $ns$ contribution to the cross-section weighted density of states is expected to be a general feature of high-energy photoemission. This promises to be of particular value in the study of conduction-band states in doped $n$-type transparent conducting oxides such as Sb-doped SnO$_2$ (Ref. 19) and Sn-doped In$_2$O$_3$ (Ref. 20). The conduction bands for these technologically important materials have dominant metal 5$s$ character and can be observed only as very weak features in conventional photoemission spectra. We anticipate that

HXPS will provide vastly superior conduction-band data for these and related materials. At the same time, HXPS will enable identification of the regions of O $2p$ valence bands that are hybridized with cation $s$ states for any oxide.

UK EPSRC supports the NCESS facility. The Boston University program is supported in part by the U.S. Department of Energy under DE-FG02-98ER45680. The Advanced Light Source is supported by the Director, Office of Science, Office of Basic Energy Sciences of the U.S. Department of Energy under Contract No. DE-AC02-05CH11231. The Trinity College Dublin program is supported by the HEA under a cycle III PRTLI award.

---

*Corresponding author. Electronic address: russell.egdell@chem.ox.ac.uk

[1] R. D. Shannon and R. X. Fischer, Phys. Rev. B **73**, 235111 (2006).

[2] *Semiconductors. Physics of Non-Tetrahedrally Bonded Binary Compounds II*, edited by O. Madelung, Landolt-Börnstein, New Series, Group III, Vol. 17, Pt. f (Springer, Berlin, 1984).

[3] W. Mindt, J. Electrochem. Soc. **116**, 1076 (1969).

[4] P. T. Moseley, J. L. Hutchison, and M. A. M. Bourke, J. Electrochem. Soc. **129**, 876 (1982).

[5] R. M. Dell and D. A. J. Rand, *Understanding Batteries* (Royal Society of Chemistry, Cambridge, 2001).

[6] M. Heinemann, H. J. Terpstra, C. Haas, and R. A. deGroot, Phys. Rev. B **52**, 11740 (1995).

[7] J. P. Pohl and G. L. Schlechtriemen, J. Appl. Electrochem. **14**, 521 (1984).

[8] H. Namatame, A. Fujimori, H. Takagi, S. Uchida, F. M. F. deGroot, and J. C. Fuggle, Phys. Rev. B **48**, 16917 (1993).

[9] B. B. Van Aken, T. T. M. Palstra, A. Filippetti, and N. A. Spalding, Nat. Mater. **3**, 164 (2004).

[10] M. Sacchi, F. Offi, P. Torelli, A. Fondacaro, C. Spezzani, M. Cautero, G. Cautero, S. Huotari, M. Grioni, R. Delaunay, M. Fabrizioli, G. Vanko, G. Monaco, G. Paolicelli, G. Stefani, and G. Panaccione, Phys. Rev. B **71**, 155117 (2005).

[11] D. J. Payne, R. G. Egdell, W. Hao, J. S. Foord, A. Walsh, and G. W. Watson, Chem. Phys. Lett. **411**, 181 (2005).

[12] D. J. Payne, R. G. Egdell, A. Walsh, G. W. Watson, J. Guo, P. A. Glans, T. Learmonth, and K. E. Smith, Phys. Rev. Lett. **96**, 157403 (2006).

[13] G. Paolicelli, A. Fondacaro, F. Offi, G. Stefani, G. Cautero, M. Cautero, B. Krastanov, P. Lacovig, P. Pittana, R. Sergo, R. Tommasini, P. Torelli, M. Sacchi, M. Grioni, G. Monaco, and G. Panaccione, J. Electron Spectrosc. Relat. Phenom. **144**, 963 (2005).

[14] G. Panaccione, G. Cautero, A. Fondacaro, M. Grioni, P. Lacovig, G. Monaco, F. Offi, G. Paolicelli, M. Sacchi, G. Stefani, and P. Torelli, Nucl. Instrum. Methods Phys. Res. A **547**, 56 (2005).

[15] A. E. Taverner, C. Rayden, S. Warren, A. Gulino, P. A. Cox, and R. G. Egdell, Phys. Rev. B **51**, 6833 (1995).

[16] R. Bader, *Atoms in Molecules: A Quantum Theory* (Oxford University Press, New York, 1990).

[17] J. H. Scofield, Lawrence Livermore National Laboratory Report No. UCRL-51326, 1973 (unpublished).

[18] J. J. Yeh and I. Lindau, At. Data Nucl. Data Tables **32**, 1 (1985).

[19] P. A. Cox, R. G. Egdell, C. Harding, W. R. Patterson, and P. Tavener, Surf. Sci. **123**, 179 (1982).

[20] Y. Gassenbauer, R. Schafranek, A. Klein, S. Zafeiratos, M. Hävecker, A. Knop-Gericke, and R. Schlögl, Phys. Rev. B **73**, 245312 (2006).